

Non-intrusive Time-POD for Optimal Control of a Fixed-Bed Reactor for CO₂ Methanation

Jens Bremer* Jan Heiland** Peter Benner**
Kai Sundmacher*

* Max Planck Institute Magdeburg, Dpt. Process Systems Engineering,
Sandtorstraße 2, 39106 Magdeburg, Germany and Otto von Guericke
University Magdeburg, Chair for Process Systems Engineering,
Universitätsplatz 2, 39106 Magdeburg (Sundmacher), (e-mail:
bremerj@mpi-magdeburg.mpg.de, kai.sundmacher@ovgu.de)

** Max Planck Institute Magdeburg, Dpt. Computational Methods in
Systems and Control Theory and Otto von Guericke University
Magdeburg, Fakultät für Mathematik (e-mail:
{heiland,benner}@mpi-magdeburg.mpg.de)

Abstract: The optimization of a controlled process in a simulation without access to the model itself is a common scenario and very relevant to many chemical engineering applications. A general approach is to apply a black-box optimization algorithm to a parameterized control scheme. The success then depends on the quality of the parametrization that should be low-dimensional though rich enough to express the salient features. This work proposes using solution snapshots to extract dominant modes of the temporal dynamics of a process and use them for low-dimensional parametrizations of control functions. The approach is called proper orthogonal decomposition in time (time-POD). We provide theoretical reasoning and illustrate the performance for the optimal control of a methanation reactor.

Copyright © 2021 The Authors. This is an open access article under the CC BY-NC-ND license (<http://creativecommons.org/licenses/by-nc-nd/4.0>)

Keywords: Optimal control, Model order reduction, Proper orthogonal decomposition, Fixed-bed reactor, Carbon dioxide methanation, Nonlinear programming, Black-box model

1. INTRODUCTION

In many engineering applications, a simulation is a multi-component combination of mathematical models, discretization routines, coupling conditions, and, possibly, heuristics. All internal states and settings aside, any simulation software can be seen as a tool that maps an input u , say a set of parameters, to an output y ; cp. Figure 1 for the example of a reactor. In this scenario, the user will have control on the input u and access to the output y . The combined model that realizes the map

$$\mathbb{G}: u \mapsto y \quad (1)$$

may stay in the background – maybe because the software is closed source, maybe because working with the model or the implementation directly on a low level is not feasible.

In optimization setups, one seeks for a control u_* such that the corresponding output $y_* = \mathbb{G}(u_*)$ has certain desired properties. With \mathcal{U} denoting the set of admissible controls and \mathcal{Y} the space of the corresponding solutions, this task is formalized as the computation of solutions

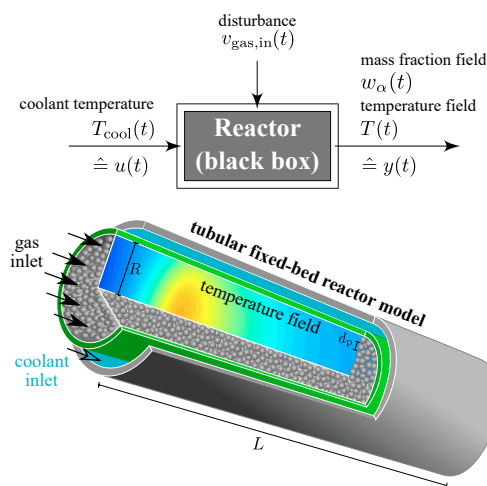
$$\mathcal{J}(\mathbb{G}(u), u) \rightarrow \min_{u \in \mathcal{U}} \quad (2)$$

where $\mathcal{J}: \mathcal{Y} \times \mathcal{U} \rightarrow \mathbb{R}$ is a suitably chosen cost functional.

If \mathcal{U} is of finite dimension k , such that any u can be parametrized via a vector $\mathbf{p} = (p_1, p_2, \dots, p_k) \in \bar{\Omega} \subset \mathbb{R}^k$ and a generating system $\{U_i\}_{i=1, \dots, k} \subset \mathcal{U}$ in terms of

$$u(\mathbf{p}) = \sum_{i=1}^k p_i U_i, \quad (3)$$

Fig. 1. Illustration of a simulation of a reactor as an input to output mapping procedure.



$$\tilde{\mathcal{J}}(\mathbf{p}) := \mathcal{J}(\mathbb{G}(u(\mathbf{p})), u(\mathbf{p})) \rightarrow \min_{\mathbf{p} \in \Omega \subset \mathbb{R}^k} . \quad (4)$$

An optimization problem like (4) can be solved by standard (black box) solvers. Apart from problem specific smoothness or convexity, the time needed to compute an approximate solution of (4) will mainly depend on

- (1) the costs of evaluating $\tilde{\mathcal{J}}(\mathbf{p})$ for a given \mathbf{p} , and
- (2) the number of control parameters k .

The presented work aims at reducing the costs through reducing k . Note that we assume that the model is not accessible, which means that also the opportunities to optimize its evaluation are restricted.

We will consider dynamical systems with single inputs and parametrizations of controls through basis functions $\{\psi_1, \dots, \psi_s\} \subset L^2(0, t_e)$ as in

$$u(t) = \sum_{i=1}^s p_i \psi_i(t) \quad (5)$$

on a time interval $(0, t_e)$. We will show that from the general considerations on space-time POD of Baumann et al. (2018), one can derive that the right-singular vectors of a matrix of snapshots of the system outputs y for some training controls provide an efficient low-dimensional basis for such parametrizations. This idea to use temporal modes of snapshots to design controls follows two principles, namely, that these modes encode patterns of time evolution (cp., e.g., Carlberg et al. (2015)) and that systems can be efficiently excited by targeting characteristic frequencies (cp., e.g., King et al. (2005)).

The approach of discretizing the control as in (5) is commonly referred to as *control parametrization*; see e.g. Goh and Teo (1988) for an early general theoretical considerations. Typically, as laid out in Lin et al. (2014), the control is discretized via a uniform time grid and through piecewise constant or linear basis functions. In Elnagar et al. (1995), the use of particular time grids has been proposed in view of provably convergent approximations with generally lower dimensions. This concept, also with more general function space parametrizations, has been applied to control batch reactors (cp., e.g., Welz et al. (2006); Aydin et al. (2018)).

Since the general need for low-dimensional parametrizations is unquestioned (cp., e.g., Alamir (2012) and the discussion in Schlegel et al. (2005)), there have been various attempts for deriving problem specific low order parametrization based on adaptive sparsification or enrichment of the underlying bases; see Schlegel et al. (2005) for an approach based on wavelets and for an overview of alternative approaches. These adaptive approaches are targeted to best resolve the optimal input for a particular optimal control problem. In contrast, the presented approach of using snapshot information is meant to provide an efficient parametrization based on system characteristics and, thus, for use in several or dynamically changing optimization setups.

We illustrate the realization and performance of this so-called time-POD based parametrization for a methanation reactor.

The optimal control of a fixed-bed reactor (FBR), as usually used for methanation, is a challenging task because of fast dynamics, high sensitivity to possible disturbances, strong nonlinearities, non-minimum phase characteristics, dead-times, and often limited control capabilities (cp., e.g., Jørgensen (1986)). Ahead of its time, Wright and Edgar (1994) introduced nonlinear model predictive control (NMPC) to the field of catalytic FBRs applied to the water-gas shift reaction. The performance of NMPC for set-point tracking of this nonlinear process was shown to be superior to conventional adaptive control, since parameter estimates varied as rapidly as the state, making successful parameter adjustment extremely difficult. Apart from that, NMPC allowed for input and state constraints simultaneously, which is often vital for practical applications and flexible reactor operation in a broad operating range. We note that the method proposed here is suitable for any control problem and thus readily included in an MPC loop. More recently, Bremer et al. (2017) considered the optimal control of an FBR start-up as a vital option to improve the reactors' heat management and, thus, to avoid hazardous reactor runaways.

This paper is structured as follows. In Section 2 and 3, we introduce the basic concepts of the time-POD approach and show how it applies for low dimensional control parametrization for general black box models. In Section 4, we describe the methanation reactor and the associated optimal control problem. In Section 5, we illustrate the numerical realization of the time-POD based control parametrization and how it performs in the optimal control of the reactor. We conclude the paper by a discussion of the results and an outlook.

2. PRELIMINARIES

We recall the basic concepts and notations of the space-time POD approach and show it provides the dominant modes of the time evolution of the states.

For illustration purposes, we will refer to a generic model of type

$$\dot{y}(t) = f(y(t), u(t)), \text{ on } (0, t_e], \quad y(0) = \alpha. \quad (6)$$

Let Y be the state space of the solutions, i.e. $y(t) \in Y$. We assume that $Y = \mathbb{R}^q$ is equipped with a suitable norm and inner product induced by a mass matrix \mathbf{M}_Y .

For fixed u , let $y \in ((0, t_e] \rightarrow Y)$ be the solution to (6). Let

$$S = \text{span}\{\psi_1, \dots, \psi_s\} \subset L^2(0, t_e)$$

be a s -dimensional space of *measurement functions* with mass matrix \mathbf{M}_S and consider the matrix of measurements

$$\mathbf{X} = \left[\int_0^{t_e} y(t) \psi_1(t) dt \dots \int_0^{t_e} y(t) \psi_s(t) dt \right] \mathbf{M}_S^{-1}, \quad (7)$$

where the k -th column is the solution y tested against ψ_k in the $L^2(0, t_e)$ inner product. This matrix defines the $L^2(0, t_e)$ -orthogonal projection \tilde{y} of y onto

$$S \cdot Y := \{h \in ((0, T] \rightarrow Y : h(t) = \sum_{k=1}^s \psi_k(t) v_k, v_k \in Y\}$$

through $\tilde{y}(t) = \sum_{k=1}^s X^{(k)} \psi_k(t)$, where $X^{(k)}$ is the k -th column of \mathbf{X} . Accordingly, depending on the *resolution* of

the time component through S , the matrix of measurements represents the function y with a certain accuracy.

In view of optimally representing \tilde{y} in a lower-dimensional time resolution, we have the following result; see (Bauermann et al., 2018, Lem. 2.7 and Sec. 4.1):

Lemma 1. The space $\hat{S} \subset S$ of dimension \hat{s} defined as $\text{span}\{\hat{\psi}_1, \dots, \hat{\psi}_{\hat{s}}\}$, where

$$\begin{bmatrix} \hat{\psi}_1 \\ \hat{\psi}_2 \\ \vdots \\ \hat{\psi}_{\hat{s}} \end{bmatrix} = V_{\hat{s}}^T (\mathbf{M}_S)^{-1/2} \begin{bmatrix} \psi_1 \\ \psi_2 \\ \vdots \\ \psi_s \end{bmatrix}, \quad (8)$$

with the matrix $V_{\hat{s}}$ of the \hat{s} leading right singular vectors of

$$(\mathbf{M}_Y)^{1/2} \mathbf{X} (\mathbf{M}_S)^{1/2},$$

is optimal in the sense that the distance of the projection $\tilde{y} \in \hat{S} \cdot Y$ to $y \in S \cdot Y$ is minimal (measured in the norm of $S \cdot Y$) over all \hat{s} -dimensional subspaces of S .

The practical implication of Lemma 1 is as follows. If the time evolution of y was well resolved by S , then \hat{S} provides an optimal low-dimensional parametrization of the time component of y . As the standard POD modes describe the preferred states of a system and provide efficient Galerkin discretizations of the space dimension, the temporal modes $\hat{\psi}_i$ encode preferred temporal dynamics and an optimal base for time Galerkin schemes.

To motivate the use of the time modes for control parametrizations, we consider a control-affine generic model of type

$$\dot{y}(t) = f(y(t)) + bu(t). \quad (9)$$

In a Galerkin time discretization on to the subspace spanned by $\{\hat{\psi}\}_{i=1, \dots, \hat{s}}$, a solution to

$$\int_0^{t_e} \hat{\psi}_i(t) \dot{y}(t) dt = \int_0^{t_e} \hat{\psi}_i(t) [f(y(t)) + bu(t)] dt, \quad (10)$$

for $i = 1, \dots, \hat{s}$, is sought. By the orthogonality property of $\hat{\psi}_i$, those parts of the control u that are not in \hat{S} will be neglected in this model. On the other hand, modes $\hat{\psi}_i$ that resonate well with $f(y(t))$ will be preserved to a high extend in this spectral discretization.

In this work we consider the single input case and the task to reduce the temporal complexity of the control. The same methodology generalizes to higher dimensions (cp. Benner and Heiland (2020)) and can be used to also reduce the spatial discretization of a distributed or multi-input control setup.

3. APPLICATION TO BLACK-BOX MODELS

In this section, we illustrate how the time-POD approach is realized for a model that only provides access to solution trajectories y for a given input u .

The general formulas of Section 2 include (factors of) the mass matrix that account for the right weighting of the components. These mass matrices might not be available in practice. For a black box model one may assume that they are the identities. This modification still leads to optimal bases but with respect to the standard

Euclidean norm as opposed to the norms that reflect the geometry and the spatial discretization. Moreover, in the case of finite difference discretization or finite volumes on a uniform tessellation, the mass matrix is the identity with a scaling factor which, however, has no effect on the computation of the modes.

The overall approach consists of three steps, namely the data acquisition, the extraction of the time modes, and the parametrization of the controls. If present, then together with the control, also the control constraints have to be parametrized.

1. Data acquisition For the initial time discretization, it is practical to define and interpret S as the nodal basis of a piecewise constant approximation on an equidistant grid

$$0 = t_0 < t_1 < \dots < t_s \quad (11)$$

so that the matrix of measurements as defined in (7) is approximated as

$$\mathbf{X} = [y(t_0) \ y(t_1) \ y(t_2) \ \dots \ y(t_s)] \in \mathbb{R}^{q \cdot s}. \quad (12)$$

Here, the approximation happens in the rough approximation of the integrals.

2. Extraction of the modes With the above time discretization, the mass matrix \mathbf{M}_S is a scaled identity and can be omitted. Then, according to Lemma 1, the time mode $\hat{\psi}$ is represented by the i -th right singular vector \mathbf{v}_i of $(\mathbf{M}_Y)^{1/2} \mathbf{X}$ in the sense that

$$\hat{\psi}_i(t) = [\mathbf{v}_i]_{\ell} \text{ on } [t_{\ell-1}, t_{\ell}], \quad \text{for } \ell = 1, \dots, s, \quad (13)$$

where $[\mathbf{v}_i]_{\ell}$ denotes the ℓ -th component of the vector \mathbf{v}_i .

3. Control parametrization With the matrix

$$\mathbf{V}_{\hat{s}} := \begin{bmatrix} \mathbf{v}_1 \\ \mathbf{v}_2 \\ \vdots \\ \mathbf{v}_{\hat{s}} \end{bmatrix} \quad (14)$$

that contains the modes as rows, a parametrized control u with $u(t) = \sum_{i=1}^{\hat{s}} p_i \hat{\psi}_i(t)$ is represented as $\mathbf{u} = \mathbf{p}^T \mathbf{V}_{\hat{s}}$.

In this representation, the inclusion of control constraints works as follows. Let \mathbf{u} be the vector that represents the control and $d\mathbf{u}$ be its (numerical) time derivative (e.g. through a finite difference approximations). Then, an upper bound $u \leq \bar{u}$ translates as

$$\mathbf{u} \leq \bar{\mathbf{u}} \leftrightarrow \mathbf{V}_{\hat{s}}^T \mathbf{p} \leq \bar{\mathbf{u}}^T \quad (15)$$

and an upper bound $\dot{u} \leq \bar{v}$ as

$$d\mathbf{u} \leq \bar{\mathbf{v}} \leftrightarrow d\mathbf{V}_{\hat{s}}^T \mathbf{p} \leq \bar{\mathbf{v}}^T, \quad (16)$$

where $d\mathbf{V}_{\hat{s}}$ contains the corresponding representations of the (numerical) approximation of $\frac{d}{dt} \hat{\psi}_i$, $i = 1, \dots, \hat{s}$.

Note that linear inequality constraints of type (15) and (16) are readily included in optimization packages.

4. EXAMPLE CASE: METHANATION REACTOR

Carbon dioxide methanation is considered an essential technological link within the Power-to-X framework, enabling the conversion of renewable electricity (e.g., from wind and solar energy) into valuable, easy-to-distribute chemical energy carriers. An exemplary process configuration is illustrated in Fig. 2 and indicates how the

intermittent availability of renewable energy influences all downstream processes. While some processes (e.g., water electrolysis) can operate at different loads without restrictions (load flexibility), other processes (e.g., methanation) require additional measures to cope with changing loads. Such measures typically include aspects of optimal dynamic operation and control (cp., e.g., Bremer et al. (2017)). However, the high complexity of the required process models often limits detailed dynamic investigations, especially for real-time control applications. Thus, non-intrusive time-POD represents a promising remedy, which will be shown in the following.

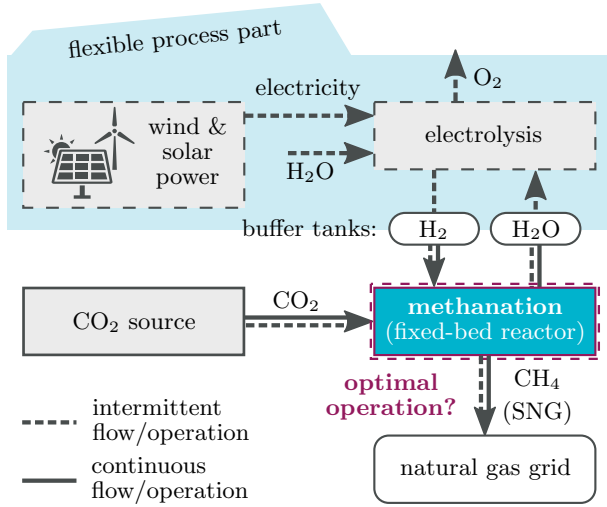
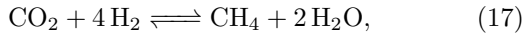


Fig. 2. Power-to-Methane process flow chart.

Let us consider the system (6) to be a dynamic fixed-bed reactor model performing the catalytic methanation of carbon dioxide



as reported by Bremer and Sundmacher (2019). This reaction is highly exothermic and very selective to methane. The required "green" hydrogen gas comes from water electrolysis, which may operate under varying loads. In consequence, the downstream methanation reactor also has to deal with changing loads, depending on the size of intermediate buffer tanks (see Fig. 2). The major challenge is that different loads inevitably impact the reactor performance and, thus, the product gas quality. In the worst case, the gas quality is insufficient or requires too much separation effort before it can be fed into the natural gas grid. Nevertheless, the reactor can be controlled by many operating parameters, which allow for significant performance improvements. However, finding the right parameter setting is tedious since it demands expensive model or data-driven optimization strategies.

4.1 Reactor Model

The reactor model's high complexity mainly originates from a coupled set of strongly nonlinear partial differential equations (PDEs), which correspond to mass and energy balances applied to the reactor interior. We can write the governing PDEs as

$$\varepsilon \rho_{\text{gas}} \frac{\partial w_\alpha}{\partial t} = -\rho_{\text{gas}} \mathbf{v} \cdot \nabla \cdot w_\alpha - \nabla \cdot \mathbf{j}_\alpha + (1 - \varepsilon) \nu_\alpha \tilde{r}, \quad (18)$$

$$(\rho c_p)_{\text{eff}} \frac{\partial T}{\partial t} = -(\rho c_p)_{\text{gas}} \mathbf{v} \cdot \nabla T - \nabla \cdot \mathbf{q} - (1 - \varepsilon) \Delta_R \tilde{H} \tilde{r},$$

where ρ is the gas density, w_α is the component mass fraction for $\alpha \in \{\text{CO}_2, \text{H}_2, \text{CH}_4, \text{H}_2\text{O}\}$, \mathbf{v} is the superficial gas velocity, \mathbf{j}_α are dispersive component fluxes, ν_α are the stoichiometric coefficients, \tilde{r} is the reaction rate of methanation, c_p is the specific heat capacity, T is the temperature, \mathbf{q} are heat fluxes, and $\Delta_R \tilde{H}$ is the heat of reaction.

When solving the 2D reactor model, several simplifications are very helpful as deeply discussed by Bremer and Sundmacher (2019). In addition to their assumptions, this work, however, only considers one (axial) spatial coordinate within the cylindrical reactor space. In the resulting 1D model, all PDE states are still strongly coupled via fluxes, mixing rules, physical properties, and empirical correlations. That is why slight disturbances (e.g., via the inlet velocity) significantly influence the reactor bed temperature field and, thus, also the reactor's productivity. We consider the conversion of carbon dioxide as the essential productivity measure, which is defined as

$$X_{\text{CO}_2}(t) = 1 - \frac{w_{\text{CO}_2, \text{out}}(t)}{w_{\text{CO}_2, \text{in}}}, \quad (19)$$

which is required to be kept as high as possible even when disturbances are present. Therefore, we consider cooling temperature as input $u(t)$ and mass fraction as well as temperature field as solution $y(t)$. Any change in the reactor load is represented by a disturbance of the inlet gas velocity $v_{\text{gas}, \text{in}}(t)$. This setup is illustrated in Fig. 1 and the corresponding reactor's reference setting in Tab. 1.

Table 1. Reactor operation and design parameter at reference state.

$p_{\text{gas}, \text{in}}$ bar(g)	$T_{\text{gas}, \text{in}}$ °C	$v_{\text{gas}, \text{in}}$ m/s	T_{cool} °C	R m	L m	d_p m
5	180	1	320	0.01	1	0.002

4.2 Problem Formulation

The control task is to operate the reactor always at its highest conversion, even under changing loads. In order to meet this demand, we formulate the following optimal control problem (OCP):

$$\begin{aligned} \max_{u(t)} \quad & \tilde{J}(u) = \frac{1}{t_e} \int_0^{t_e} X_{\text{CO}_2}(t) dt, \\ \text{s.t.} \quad & \text{reactor model:} \\ & \dot{y}(t) = f(y(t), u(t)), \text{ on } (0, t_e] \\ & y(0) = y_0, \\ & \text{constraints:} \\ & u_{\text{ub}}(t) \geq u(t) \geq u_{\text{lb}}(t), \\ & \dot{u}_{\text{ub}}(t) \geq \dot{u}(t) \geq \dot{u}_{\text{lb}}(t). \end{aligned} \quad (20)$$

Here the reactor model is represented as an ordinary differential equation (ODE) system, which results from the finite volume method applied to PDE system (18). Inequality constraints are used to incorporate technical

restrictions on states and control. For instance, we allow a maximum input change of $20^\circ\text{C}/\text{min}$, to account for the inertia of the cooling system.

4.3 The forward solution

The initial state in problem 20 is represented by an ignited reactor, operating after successful start-up at the reference state of Tab. 1. From here the reactor model, implemented in MATLAB2018a, is integrated in time via the *idas* integrator provided by the SUNDIALS suite (cp. Hindmarsh et al. (2005)). CasADi v3.5.1 (cp. Andersson et al. (2018)) is used as symbolic framework that provides the interface between MATLAB2018a and SUNDIALS.

5. BLACK-BOX OPTIMIZATION OF THE REACTOR

To compute the basis $\{\hat{\psi}_i\}_{i=1,\dots,\hat{s}}$ according to Lemma 1 and as laid out in Section 3, we compute the forward solution of the reactor model for 4 training inputs as depicted in Figure 4 (top). The resulting trajectories are stacked into the snapshot matrix \mathbf{X} as in (12). A singular value decomposition of \mathbf{X} then reveals the dominating time modes (see Figure 4) as those that are associated with the largest singular values (see Figure 3).

The performance of the reduced approach strongly depends on the design of the training inputs and the choice of the modes for the parametrization. In this application case, to account for the fast transient dynamics of the reactor, we used slowly varying training inputs. The number of modes was fixed through testing the performance of the optimization for varying model sizes.

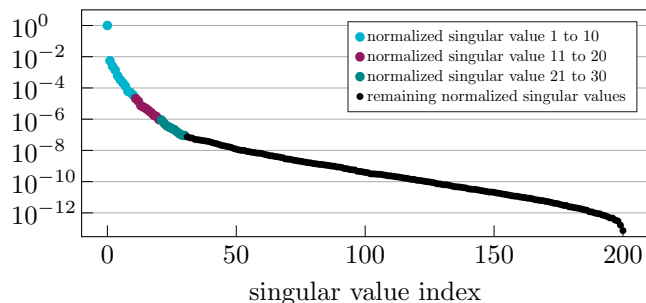


Fig. 3. Singular values of the snapshot matrix.

We set $\hat{s} = 8$ and take the \hat{s} dominant modes for parametrizing the control so that the PDE constrained optimization problem (20) is turned into a finite dimensional optimization problem (4) over \hat{s} parameters. As constraints, we apply $|\dot{u}(t)| \leq \frac{20^\circ\text{C}}{60\text{s}}$ to respect the maximal feasible change rate in the cooling temperature and $|\dot{u}(t)| \leq \epsilon \frac{20^\circ\text{C}}{60\text{s}}$, where $\epsilon = 0.1$, on the final 20s in order to enforce a convergence towards a steady state.

To solve the optimization problem for the *POD solution*, we employ the routine *ga* of MATLAB2018a which is an implementation of a *genetic algorithm*.

We compare the result of the time-POD approach the optimization of the two parameter control design

$$u(t) = \begin{cases} u_0 + \frac{p_2 - u_0}{p_1} t, & \text{if } 0 \leq t < p_1, \\ p_2, & \text{if } t \geq p_1, \end{cases} \quad (21)$$

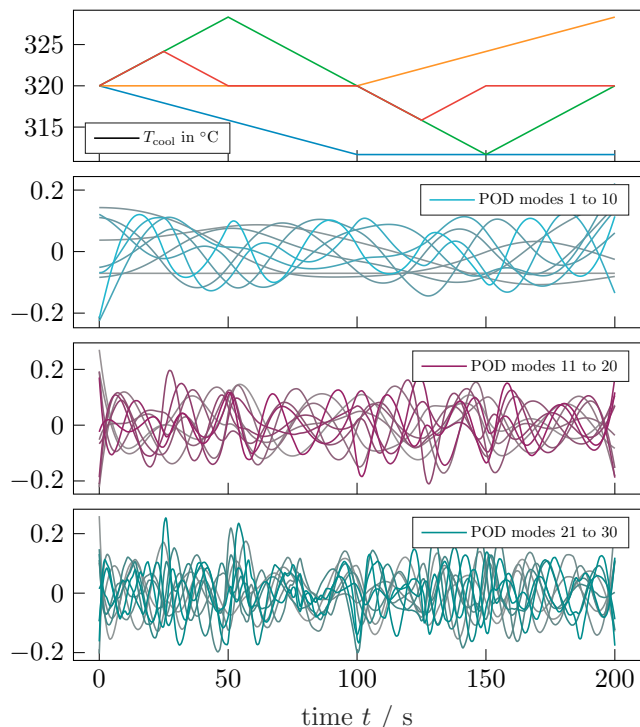


Fig. 4. Training inputs for POD snapshot generation (top) and calculated POD time modes 1 to 30.

that is motivated by the experience that the final optimal state is a steady state. The corresponding $2P$ solution is then obtained with the use of the *fmincon* routine in MATLAB2018a that realizes an interior point method. The compliance with the maximal change rate is enforced through an inequality constraint on p_1 and p_2 .

Despite the different control trajectories, both approaches maximized the cost function in (20), since the conversion of carbon dioxide is increased by the end of the time horizon. This indicates that the time-POD approach delivers valid optimal control trajectories that can be applied to the presented example case. Further improvements may be necessary to ensure a better convergence to an optimal level towards the end of the simulation.

It is well-known for standard POD approximations, the time-POD parametrization approach might perform better for problems with more diffusivity. In the considered setup, with fast reactive dynamics, the discrepancy between oscillatory modes (cp. Figure 4) and the trend of optimal controls to constant levels (cp. Figure 5) is challenging for an optimization algorithm. In fact, the optimization was significantly governed by the constraints and possibly faster, gradient based optimization methods got stuck in local minima in our investigations. Still, as the example shows, the consideration of more dynamic controls may ensure a high productivity level under changing conditions.

6. DISCUSSION AND CONCLUSION

We have presented an automated data-based approach to control parametrizations for the optimal control of black-box models. In the application for the optimization of a methanation reactor, this time-POD parametrization delivered a comparable performance improvement as a

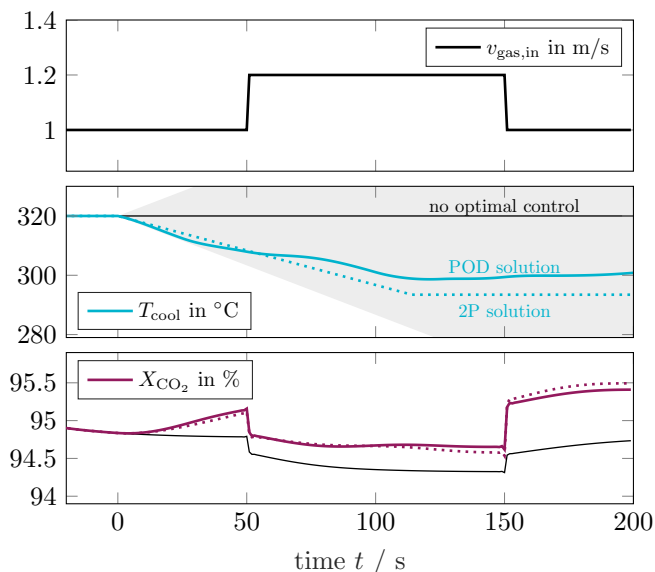


Fig. 5. The trajectory of the changing reactor load via $v_{\text{gas,in}}$ (top), the considered controls with feasible region shaded in gray (center), and resulting conversion rates (bottom).

heuristic low-dimensional approach that included a priori knowledge. Curiously, the optimal control trajectories of both approaches slightly differ which indicates further potential for optimization.

In order to react to unknown perturbations, a feedback approach is mandatory. The time-POD parametrization provides an ansatz for an open-loop control that, without further modification, can also be included in an MPC loop for closed-loop control of reactors (Durand et al. (2016)). In particular in such a setup, improvements can be expected from updating the time-POD basis as it is done in standard POD in optimization contexts as explained, e.g., in Kunisch and Volkwein (2008).

REFERENCES

- Alamir, M. (2012). A framework for real-time implementation of low-dimensional parameterized NMPC. *Automatica*, 48(1), 198–204. doi:10.1016/j.automatica.2011.09.046.
- Andersson, J.A.E., Gillis, J., Horn, G., Rawlings, J.B., and Diehl, M. (2018). CasADi – A software framework for nonlinear optimization and optimal control. *Mathematical Programming Computation*.
- Aydin, E., Bonvin, D., and Sundmacher, K. (2018). Toward fast dynamic optimization: An indirect algorithm that uses parsimonious input parameterization. *Industrial & Engineering Chemistry Research*, 57(30), 10038–10048. doi:10.1021/acs.iecr.8b02109.
- Baumann, M., Benner, P., and Heiland, J. (2018). Space-time Galerkin POD with application in optimal control of semi-linear parabolic partial differential equations. *SIAM J. Sci. Comput.*, 40(3), A1611–A1641. doi:10.1137/17M1135281.
- Benner, P. and Heiland, J. (2020). Space and chaos-expansion Galerkin POD low-order discretization of PDEs for uncertainty quantification. e-print 2009.01055, arXiv. URL <http://arxiv.org/abs/2009.01055>.
- Bremer, J., Rätze, K.H.G., and Sundmacher, K. (2017). CO₂ Methanation: Optimal Start-Up Control of a Fixed-Bed Reactor for Power-To-Gas Applications. *AIChE Journal*, 63(1), 23–31. doi:10.1002/aic.15496.
- Bremer, J. and Sundmacher, K. (2019). Operation range extension via hot-spot control for catalytic CO₂ methanation reactors. *Reaction Chemistry & Engineering*, 69(2015), 613. doi:10.1039/C9RE00147F.
- Carlberg, K., Ray, J., and van Bloemen Waanders, B. (2015). Decreasing the temporal complexity for nonlinear, implicit reduced-order models by forecasting. *Comp. Meth. Appl. Mech. Eng.*, 289, 79–103.
- Durand, H., Ellis, M., and Christofides, P.D. (2016). Economic model predictive control designs for input rate-of-change constraint handling and guaranteed economic performance. *Comput. Chem. Eng.*, 92, 18 – 36. doi:10.1016/j.compchemeng.2016.04.026.
- Elnagar, G., Kazemi, M.A., and Razzaghi, M. (1995). The pseudospectral Legendre method for discretizing optimal control problems. *IEEE Transactions on Automatic Control*, 40(10), 1793–1796. doi:10.1109/9.467672.
- Goh, C.J. and Teo, K.L. (1988). Control parametrization: A unified approach to optimal control problems with general constraints. *Automatica*, 24(1), 3–18. doi:10.1016/0005-1098(88)90003-9.
- Hindmarsh, A.C., Brown, P.N., Grant, K.E., Lee, S.L., Serban, R., Shumaker, D.E., and Woodward, C.S. (2005). SUNDIALS: Suite of nonlinear and differential/algebraic equation solvers. *ACM Transactions on Mathematical Software (TOMS)*, 31(3), 363–396.
- Jørgensen, S.B. (1986). Fixed Bed Reactor Dynamics and Control - A Review. *IFAC Proceedings Volumes*, 19(15), 11–24. doi:10.1016/S1474-6670(17)59393-3.
- King, R., Seibold, M., Lehmann, O., Noack, B.R., Morzyński, M., and Tadmor, G. (2005). Nonlinear flow control based on a low dimensional model of fluid flow. In T. Meurer, K. Graichen, and E.D. Gilles (eds.), *Control and Observer Design for Nonlinear Finite and Infinite Dimensional Systems*, 369–386. Springer. doi:10.1007/11529798_23.
- Kunisch, K. and Volkwein, S. (2008). Proper orthogonal decomposition for optimality systems. *ESAIM: Math. Model. Numer. Anal.*, 42(1), 1–23.
- Lin, Q., Loxton, R., and Teo, K.L. (2014). The control parameterization method for nonlinear optimal control: A survey. *Journal of Industrial & Management Optimization*, 10, 275–309. doi:10.3934/jimo.2014.10.275.
- Schlegel, M., Stockmann, K., Binder, T., and Marquardt, W. (2005). Dynamic optimization using adaptive control vector parameterization. *Comp. Chem. Eng.*, 29(8), 1731 – 1751. doi:10.1016/j.compchemeng.2005.02.036.
- Welz, C., Srinivasan, B., Marchetti, A., Bonvin, D., and Ricker, N.L. (2006). Evaluation of input parameterization for batch process optimization. *AIChE Journal*, 52(9), 3155–3163. doi:10.1002/aic.10905.
- Wright, G.T. and Edgar, T.F. (1994). Nonlinear model predictive control of a fixed-bed water-gas shift reactor: An experimental study. *Comput. Chem. Eng.*, 18(2), 83–102. doi:10.1016/0098-1354(94)80130-4.